

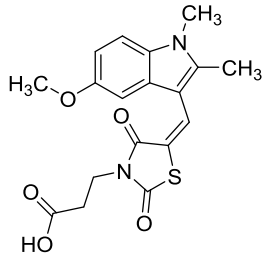
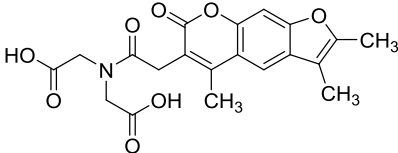
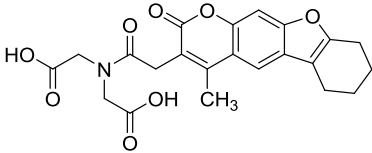
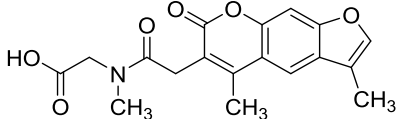
Supplementary data

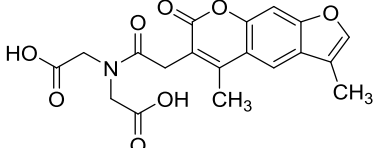
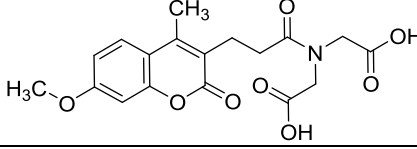
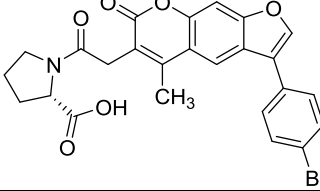
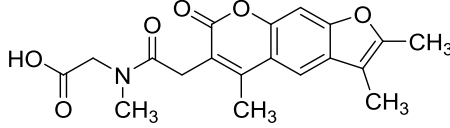
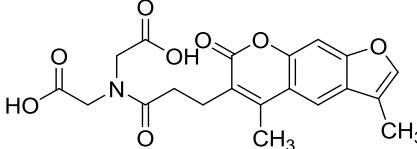
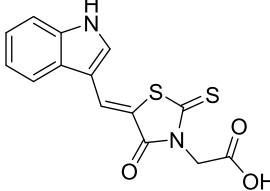
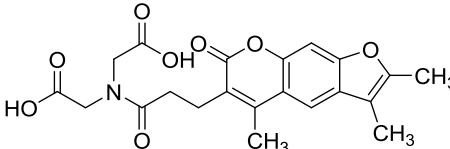
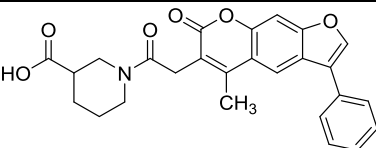
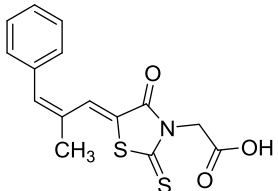
Table S1. Auto-pharmacophore generated best hypotheses for epalrestat and HNE.

Generated hypotheses	Features (ALR2; Epalrestat)	Features (ALR1; HNE)
Pharmacophore 1	3HBA, 1H, 1NI, 1RA	1HBA, 1HBD, 1H
Pharmacophore 2	3HBA, 2H, 1NI	1HBA, 1HBD, 1H
Pharmacophore 3	2HBA, 1H, 1NI, 1RA	2HBA, 1H
Pharmacophore 4	2HBA, 2H, 1NI	2HBA, 1H
Pharmacophore 5	3HBA, 1NI, 1RA	-
Pharmacophore 6	3HBA, 1H, 1NI	-
Pharmacophore 7	2HBA, 1H, 1NI, 1RA	-
Pharmacophore 8	2HBA, 2H, 1NI	-
Pharmacophore 9	3HBA, 1H, 1NI	-
Pharmacophore 10	2HBA, 2H, 1NI	-

HBA = Hydrogen bond acceptor, HBD = Hydrogen bond donor, H = Hydrophobic, NI = Negative ionizable, RA = Ring aromatic

Table S2. PAINS filter results, docking scores and binding affinities of 12 hits with the catalytic domain of ALR1 (3H4G).

Sr. No	Compound ID	Structure	PAINS filter	CDOCKER energy (kcal/mol)	CDOCKER interaction energy (kcal/mol)	Binding energy (MM-GBSA score, kcal/mol)	Key interactions
5	STOCK1N-88220		Passed	-16.78	-38.83	-35.19	Trp22, Met302, Arg312
7	STOCK1N-44092		Passed	-24.13	-45.09	-48.14	Lys23
8	STOCK1N-46096		Passed	-11.35	-38.45	-47.67	Lys23
9	STOCK1N-44771		Passed	-21.54	-40.53	-39.89	Trp22, Lys23

11	STOCK1N-44713		Passed	-28.90	-42.91	-42.07	Lys23, Ala219
12	STOCK1N-46041		Passed	-28.55	-44.37	-30.99	Lys127, Arg312
13	STOCK1N-59369		Passed	ND*	ND*	ND*	ND*
14	STOCK1N-43987		Passed	-23.95	-46.00	-35.60	Trp22, Arg312
19	STOCK1N-57572		Passed	-26.67	-41.40	-53.59	Lys23, Ala219
20	STOCK1N-31184		Failed	-11.04	-28.45	-38.35	-
23	STOCK1N-46421		Passed	-35.55	-46.55	-59.89	Lys127, Arg312
30	STOCK1N-69620		Passed	-11.47	-43.73	-53.19	Lys23
	Epalrestat		Failed	-16.94	-47.90	-65.13	Lys127

*Not Docked (ND)

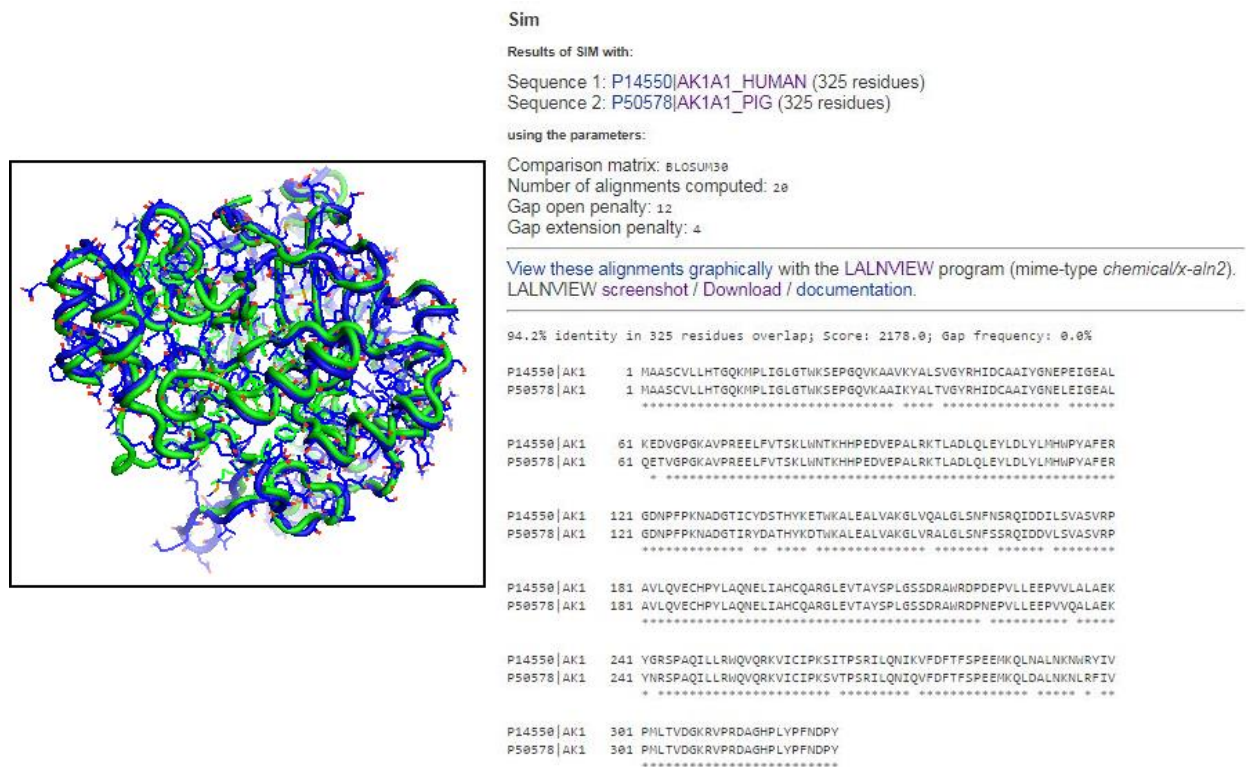


Figure S1. Aligned pose of ALR1 enzyme from porcine, in green; Homo sapiens, in blue (left) and similarity search data generated with SIM webserver (right).

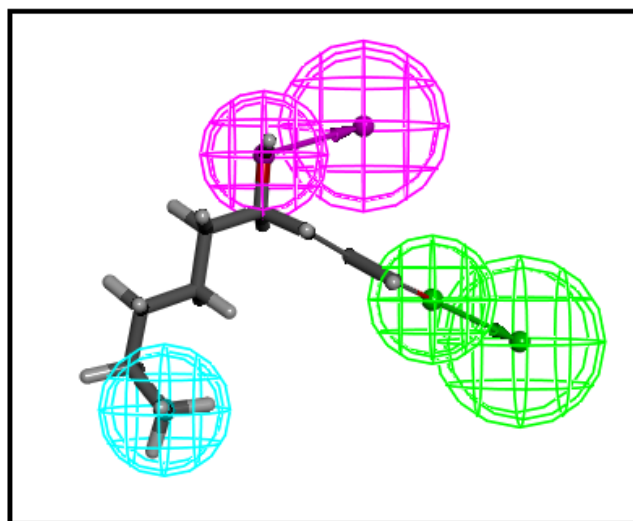


Figure S2. HNE mapped auto-pharmacophore showing key pharmacophoric features.

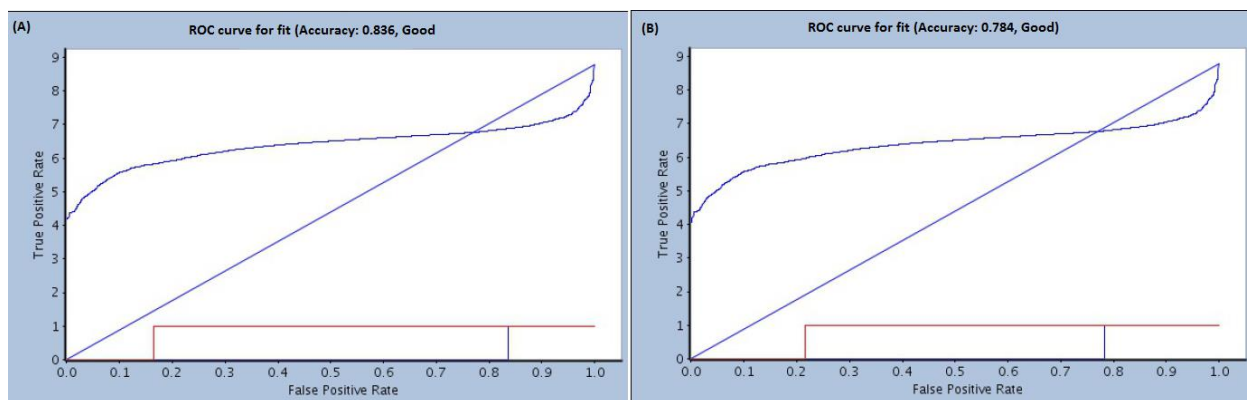


Figure S3. AUC score calculated on the basis of ROC analysis of the auto-pharmacophore of epalrestat (A) and HNE (B).

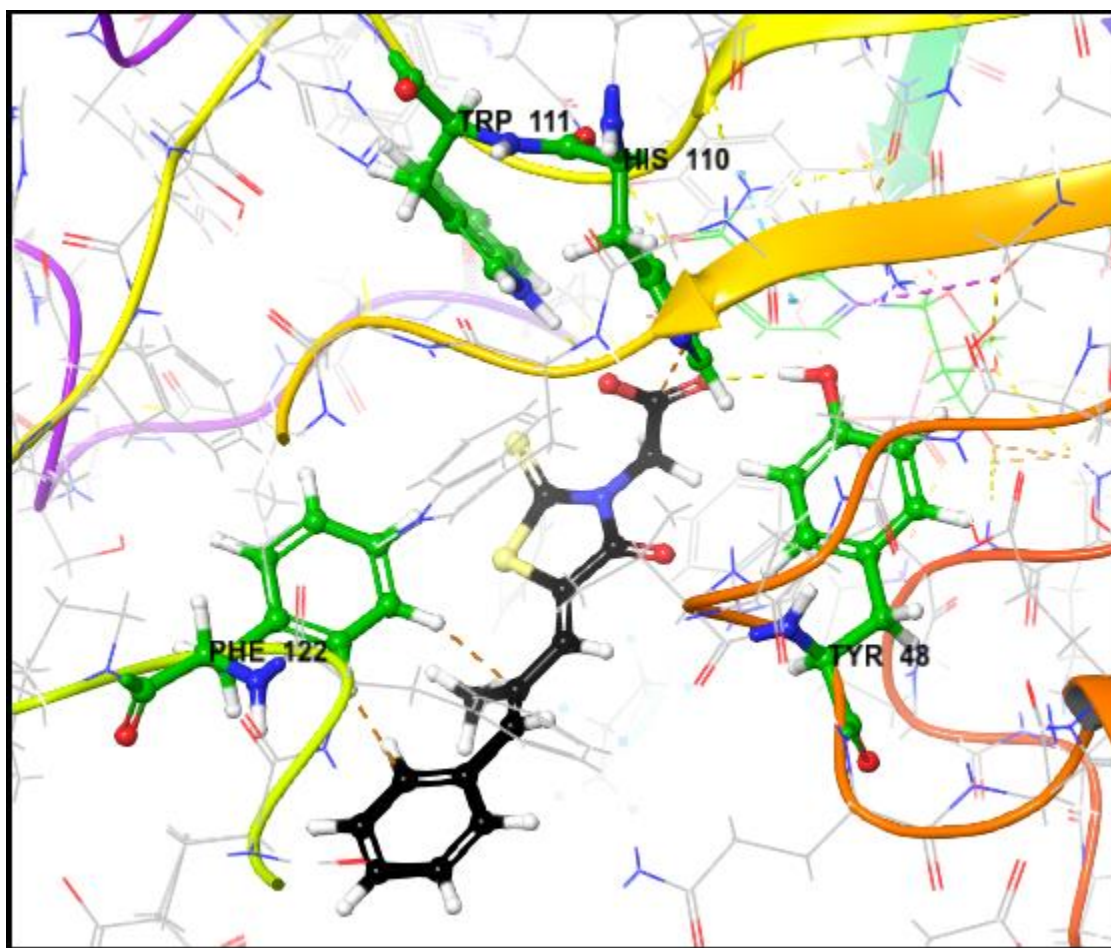


Figure S4. Docking pose showing key residue interaction of epalrestat with ALR2 protein.

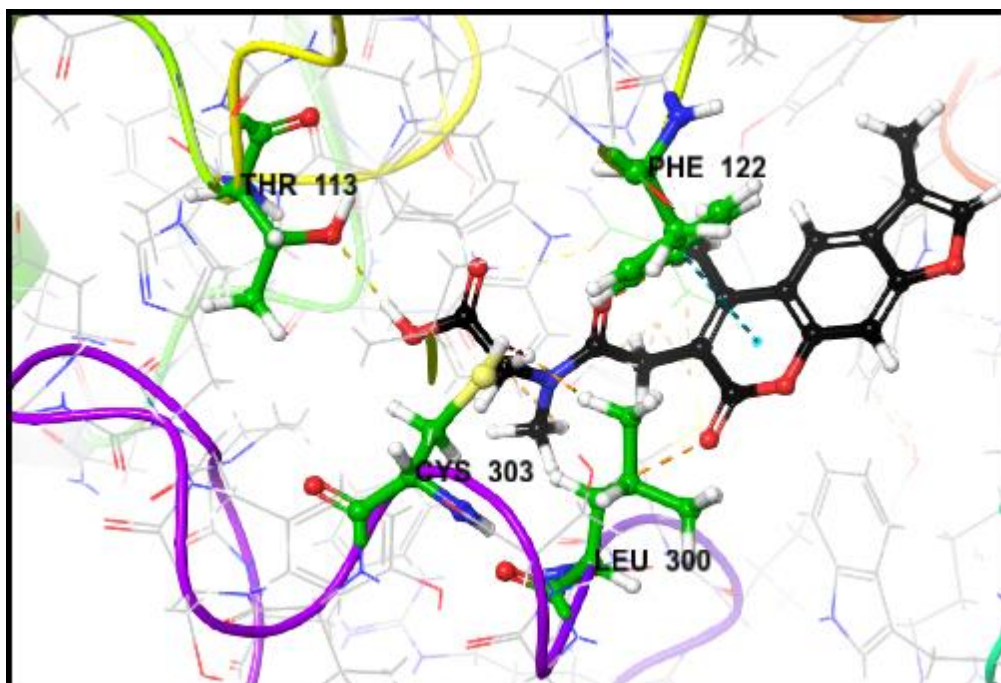


Figure S5. Docking pose showing key residue interaction of STOCKIN-44771 with ALR2 protein.

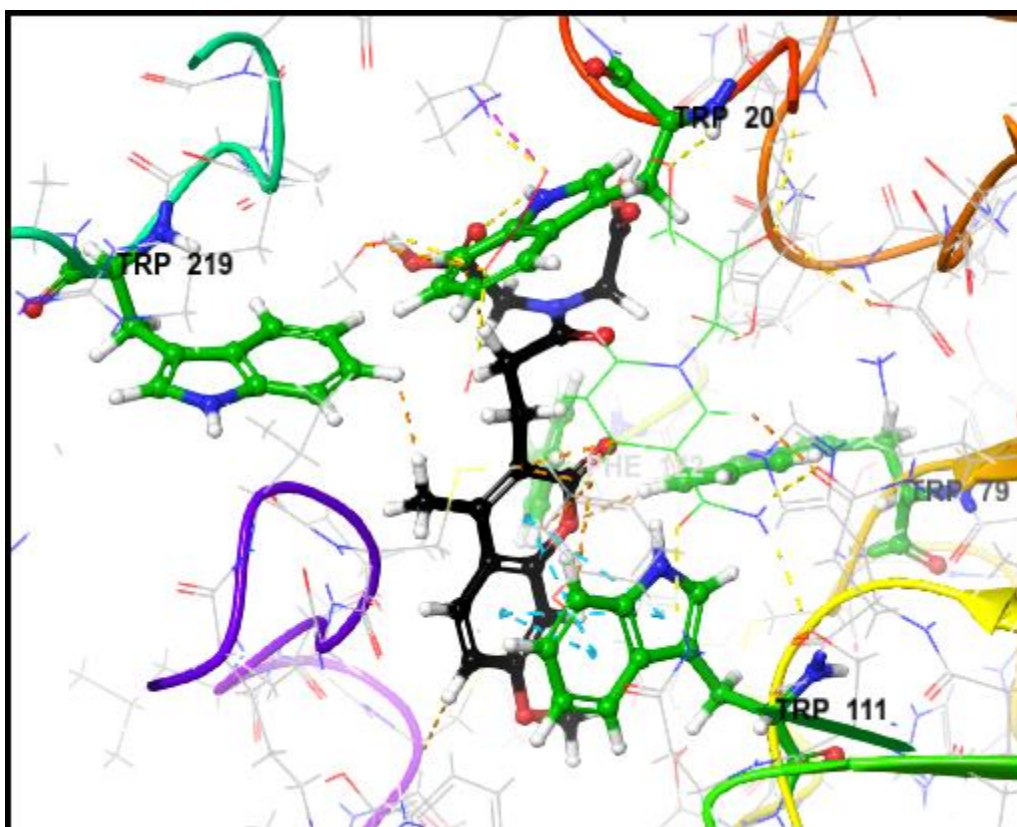


Figure S6. Docking pose showing key residue interaction of STOCKIN-46041 with ALR2 protein.

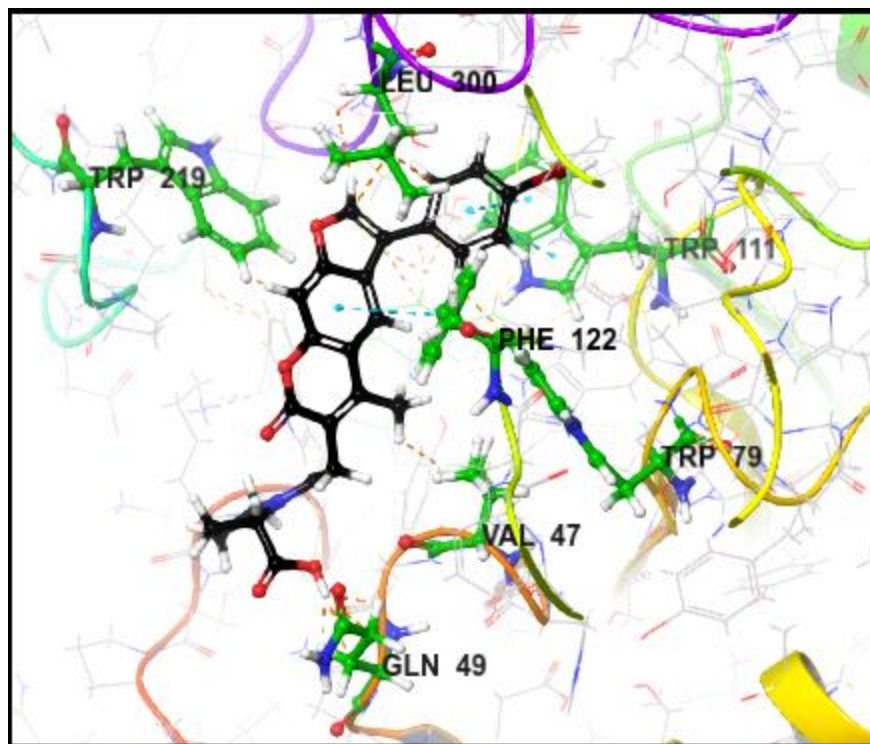


Figure S7. Docking pose showing key residue interaction of STOCKIN-59369 with ALR2 protein.

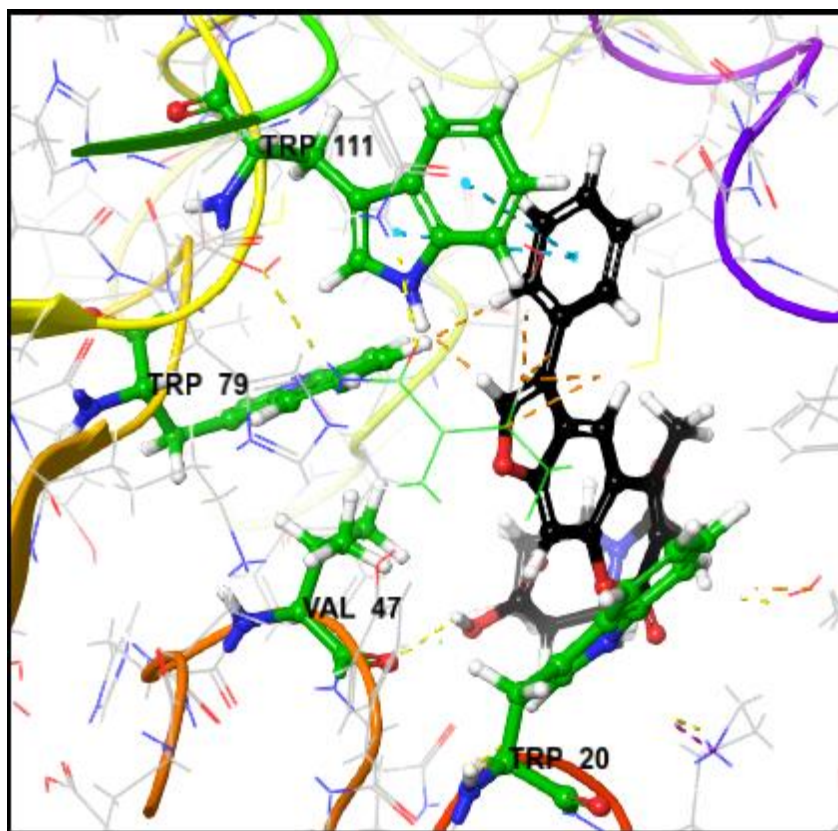


Figure S8. Docking pose showing key residue interaction of STOCKIN-69620 with ALR2 protein.

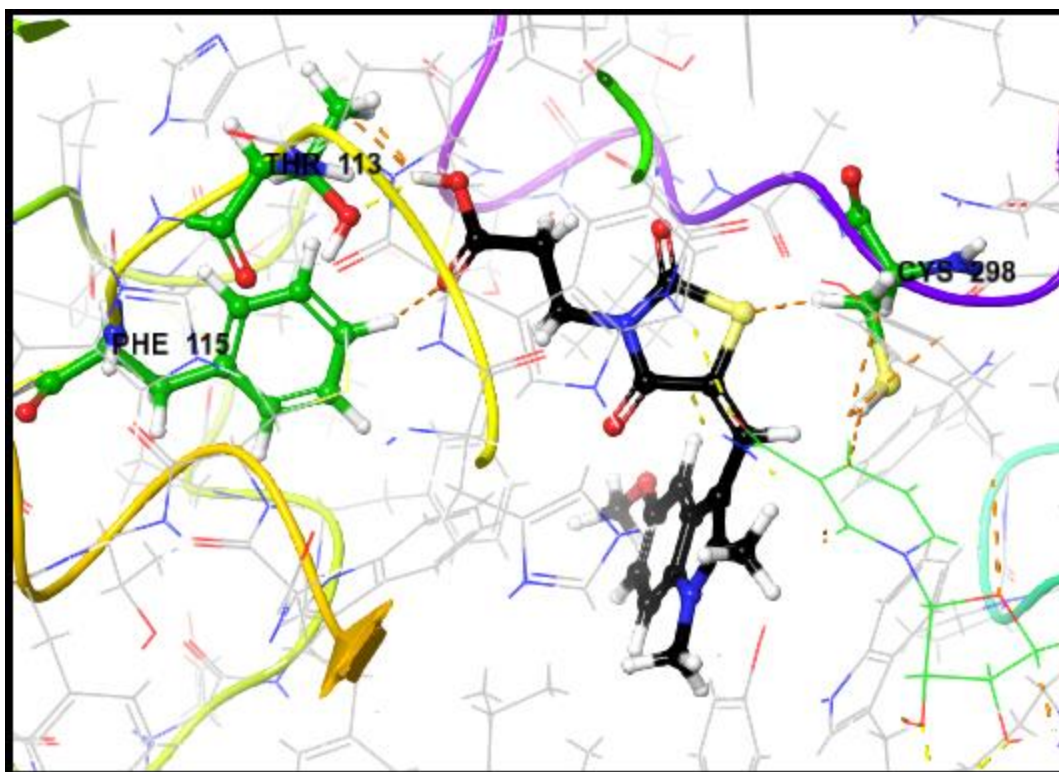


Figure S9. Docking pose showing key residue interaction of STOCKIN-88220 with ALR2 protein.

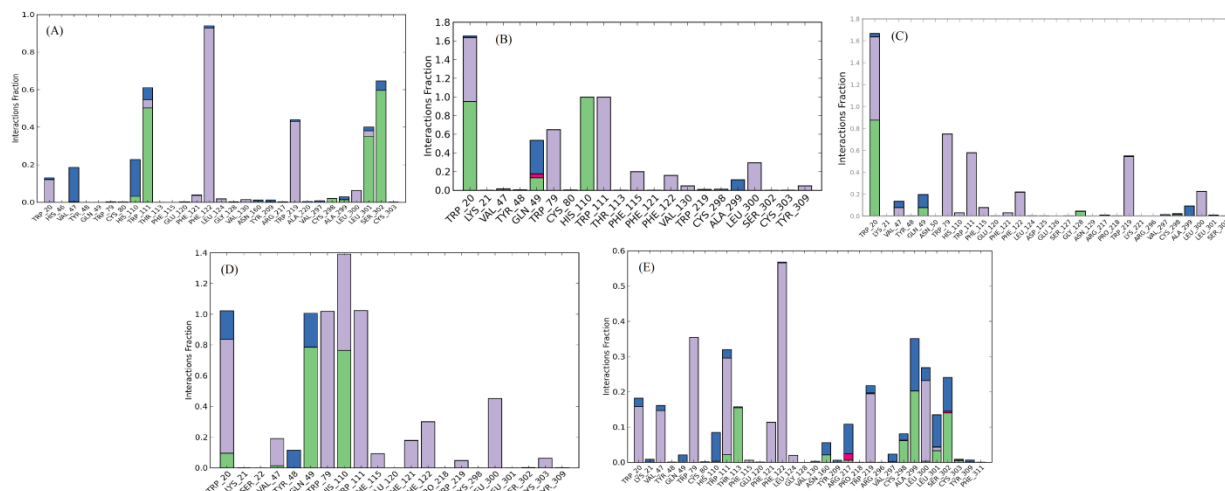


Figure S10. Histogram representing the interaction fractions of top five hits (A) STOCKIN-44771, (B) STOCKIN-46041, (C) STOCKIN-59369, (D) STOCKIN-69620, (E) STOCKIN-88220 in the catalytic domain of ALR2 throughout the simulation period of 50 ns.

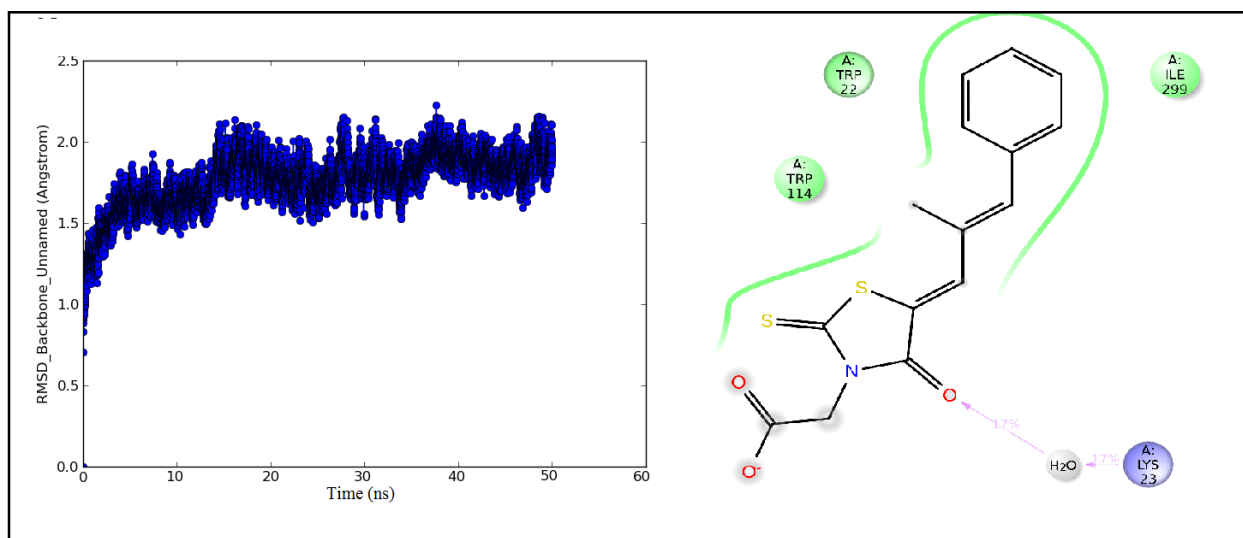


Figure S11. RMSD plot and contact summary of ALR1-Epalrestat complex throughout the simulation period of 50 ns.

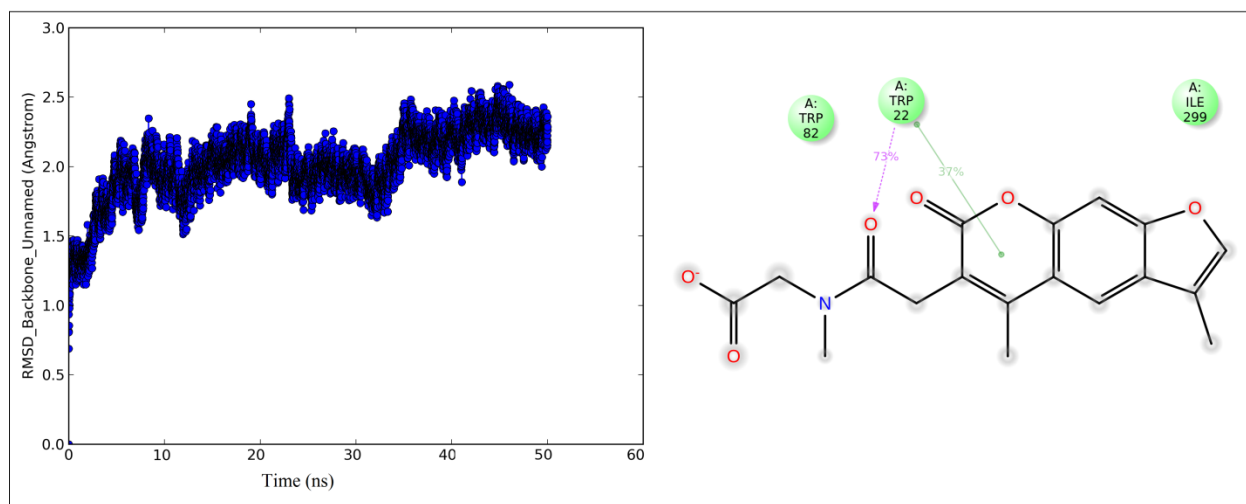


Figure S12. RMSD plot and contact summary of ALR1-44771 complex throughout the simulation period of 50 ns.

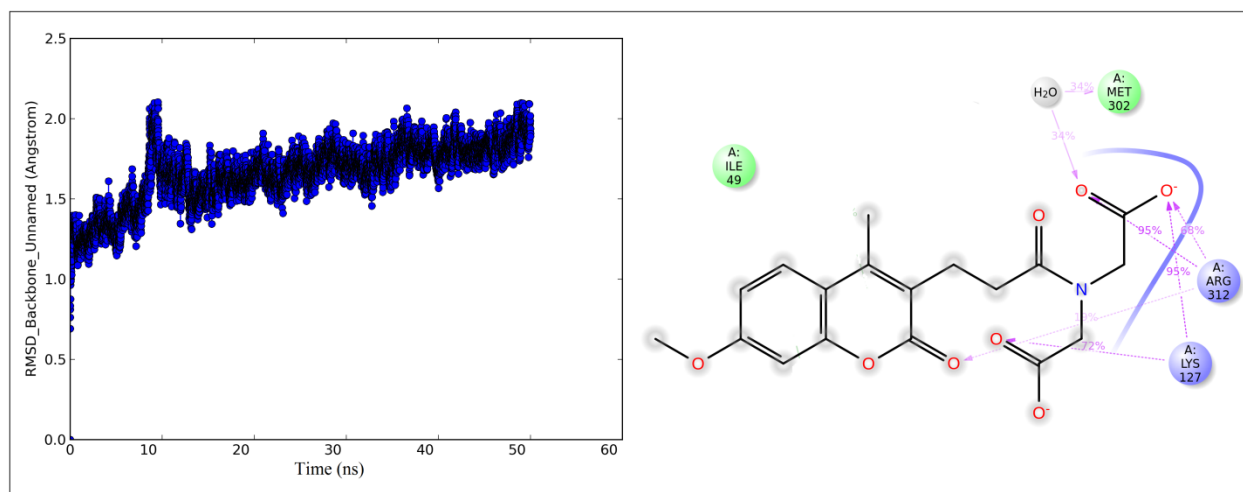


Figure S13. RMSD plot and contact summary of ALR1-46041 complex throughout the simulation period of 50 ns.

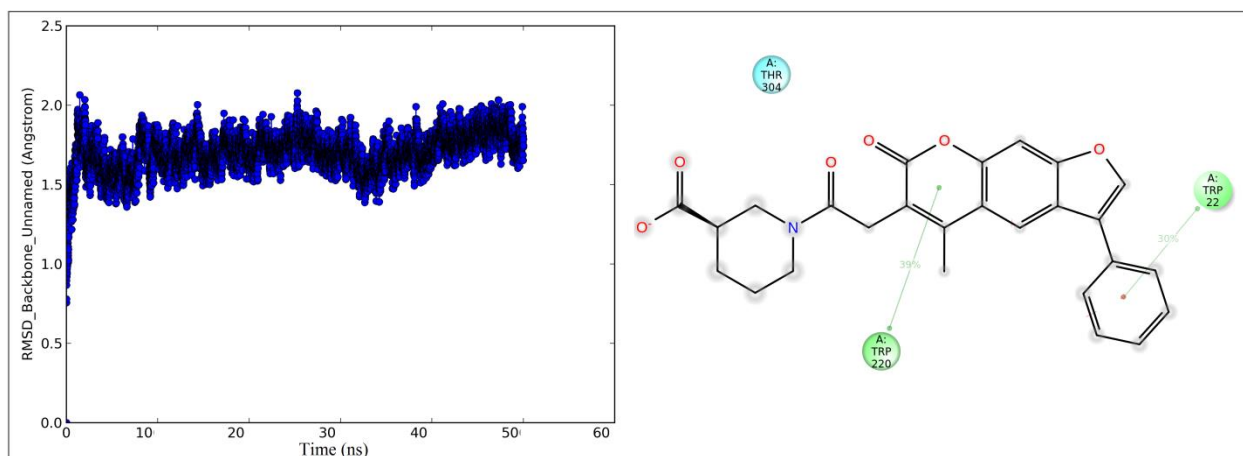


Figure S14. RMSD plot and contact summary of ALR1-69620 complex throughout the simulation period of 50 ns.

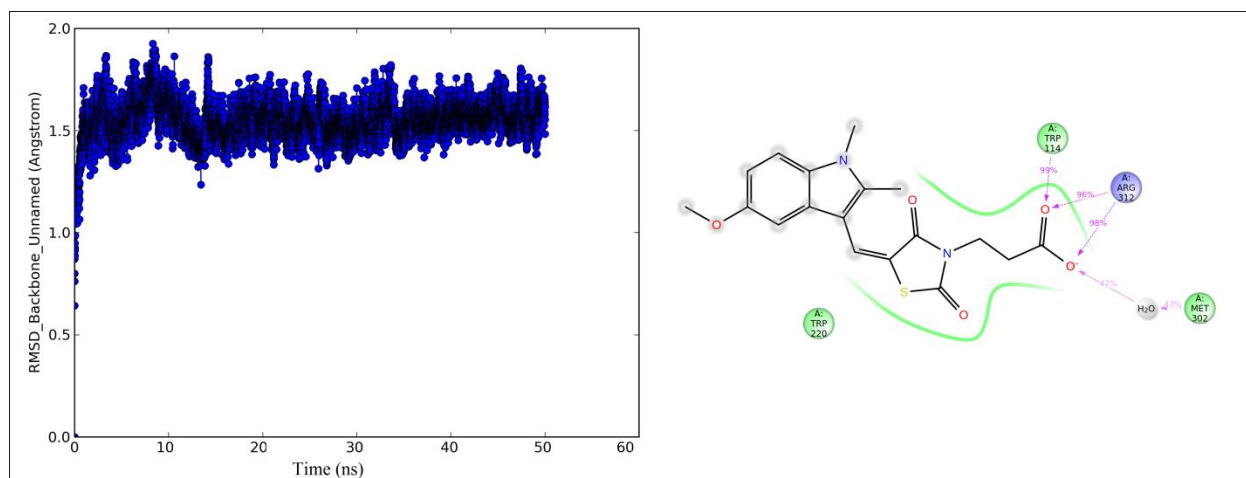


Figure S15. RMSD plot and contact summary of ALR1-88220 complex throughout the simulation period of 50 ns.